

**Magneto Optical Trapping of Rb 87**

By

**Connor Awe**

Defended on 04/07/2015

**Defense Committee**

Thesis Advisor: Dr. Steve Cundiff - Physics

Honors Council Representative: Dr. Jun Ye - Physics

Outside Department Representative: Dr. Christine Kelly – Chemistry

Awe, Connor (Honors, Physics).

*“Magneto Optical Trapping of Rubidium 87”*

Thesis Advisor Steve Cundiff

### **Abstract**

Magneto optical traps brilliantly combine semi-classical optics with modern physics. By carefully controlling the polarization and frequency of laser beams, it is possible to trap and cool atoms down to the millikelvin range at a relatively low cost. This has opened previously inaccessible physical domains to enterprising physicists all around the world, and is responsible for some of the most interesting experiments being conducted in AMO sciences today. We attempted to employ magneto optical trapping techniques to generate a sample of Rubidium 87 atoms for use in the development of multidimensional Fourier transform spectroscopy with comb lasers. My work entailed the construction and characterization of two external cavity diode lasers (ECDLs), as well as the assembly of a MOT system, which is as of 04/07/2015 not operational. Future work will focus on debugging the system.

## Table of Contents

<b>MAGNETO OPTICAL TRAPPING OF RB 87</b>	<b>1</b>
<hr/>	
<b>ABSTRACT</b>	<b>2</b>
<hr/>	
<b>DEDICATION</b>	<b>4</b>
<hr/>	
<b>MOTIVATION</b>	<b>5</b>
<hr/>	
<b>MOT THEORY AND BACKGROUND</b>	<b>8</b>
<hr/>	
<b>1) HISTORY OF THE MOT</b>	<b>8</b>
<b>2) LASER COOLING</b>	<b>8</b>
2.1 THE OPTICAL DOPPLER EFFECT	8
2.2 THE LIGHT FORCE	9
2.3 DARK STATE TRANSITIONS AND THE REPUMP LASER	11
<b>3) MAGNETIC TRAPPING AND THE ZEEMAN EFFECT</b>	<b>12</b>
3.1 THE ZEEMAN EFFECT	13
3.2 POLARIZATION STATES	15
<b>4) EXTERNAL CAVITY DIODE LASERS (ECDLS)</b>	<b>16</b>
4.1) BASIC PICTURE	16
4.2) LITTROW CONFIGURATION	17
4.3) FREQUENCY STABILIZATION AND SATURATED ABSORPTION SPECTROSCOPY	18
4.4) MODE HOPPING	25
<hr/>	
<b>MOT CONSTRUCTION AND CHARACTERIZATION</b>	<b>28</b>
<hr/>	
<b>5) CONSTRUCTION AND CHARACTERIZATION OF THE ECDLS</b>	<b>28</b>
5.1) THE TRAPPING LASER	29
5.2) THE REPUMP LASER	30
5.3) CONFIGURATION OF THE LASER INTO THE MOT	30
5.4) THE MOT CHAMBER	31
<hr/>	
<b>CONCLUSIONS AND FUTURE WORK</b>	<b>32</b>
<hr/>	
<b>REFERENCES</b>	<b>32</b>
<hr/>	

## **Dedication**

To my family, who have made my physics career possible. And to Kenny, I miss you  
boy.

Special thanks to Dr. Steve Cundiff, Dr. Bacha Lomsadze, and the entire Cundiff Lab for giving me the opportunity to work and learn with them. You each taught me a great deal and made my time in JILA both fun and productive. I'll miss you all.

## **Motivation**

I've undertaken my research in support of Dr. Bachana Lomsadze's work to improve multidimensional Fourier transform spectroscopy. Multidimensional Fourier transform spectroscopy is a complex technique, and I shall only attempt to give a very broad overview of the subject to provide some context for my work. In standard two-dimensional Fourier transform spectroscopy; we would hit a sample of interest with three pulses of laser light. We call the delay between the first and second pulses  $T$  and the delay between the second and third pulses  $\tau$ . The first pulse polarizes the sample so that it is in a superposition of ground and excited states. The second pulse achieves a population inversion, so that the sample is purely in the excited state, and the third pulse puts the sample back into a superposition state. The pulse train is shown in figure 1.

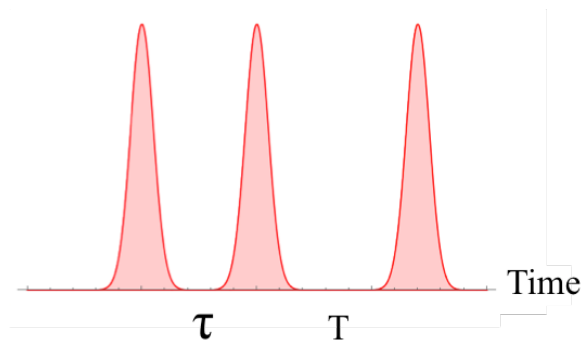


Fig. 1 – Three pulses of standard 2D spectroscopy. My work.

While the sample is polarized (between the first and second pulses and then after the third pulse), it will radiate and we obtain a spectrum from the sample. To generate a 2D spectrum, we vary the delays  $T$  and  $\tau$ , and take the Fourier transforms of the spectra we obtain with respect to  $T$  and  $\tau$ . This yields a plot with axes  $\omega_T$  and  $\omega_\tau$  with peaks indicating the frequencies at which the sample absorbs/emits light. Figure 2 gives two such plots.

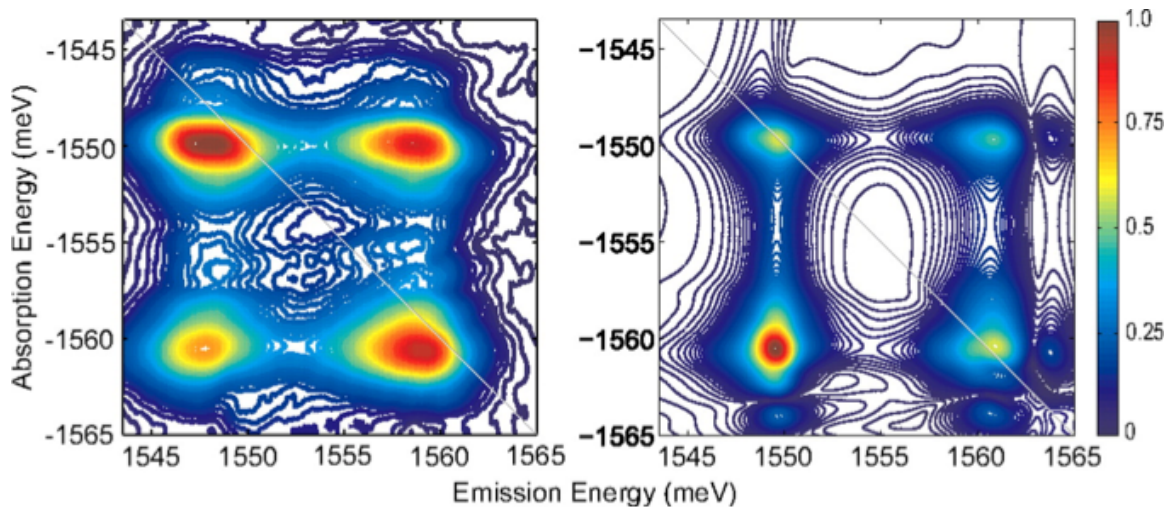


Fig. 2 - Two dimensional Fourier transform spectroscopy. [1].

Note that the absorption energy axis is negative, so that peaks on the marked diagonal line indicate that the sample absorbs and emits at the same frequency. Taking a slice along the diagonal line would yield a standard 1D spectrum. The off-diagonal peaks (which are not present in a one dimensional spectrum) indicate coupling between the diagonal peaks, and it is this feature of 2D spectroscopy that is most useful. Off-diagonal peaks allow us to distinguish between a system with multiple excited states and several systems each with their own excited states. As an example, consider the difference between two two-level systems and one three-level system, as shown in figure 3.

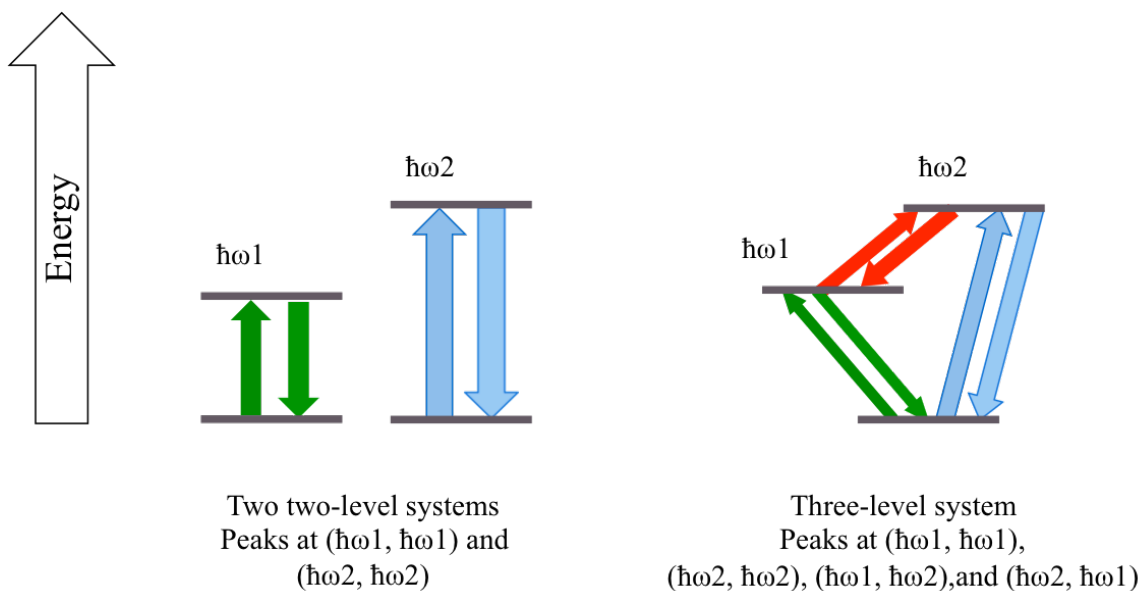


Fig. 3 – Two two-level systems vs. One three-level system. My work.

In the case of the two two-level systems, there would be no off-diagonal peaks in the 2D spectrum, because it is not possible for either atom to absorb or emit at the other's resonant frequency. However, in the case of a three level system, there will be off-diagonal peaks because the system is free to absorb at one frequency but emit at another as it transitions between the ground state, first excited state, and second excited state. The ability to distinguish between two systems with similar one-dimensional spectra has many possible applications, particularly to the detection of dangerous chemicals. Dr. Lomsadze's current research is focused on performing 2D spectroscopy with a comb laser. The technique differs from standard 2D spectroscopy in other ways (primarily in replacing three pulses with two and scanning the positions of comb lines in frequency space rather than a pulse delay, see figure 4), and is still largely theoretical. But Dr. Lomsadze hopes that the lines of a comb laser will provide better resolution than the relatively broad pulses that are normally used. My MOT is meant to provide Dr. Lomsadze with a very cold sample to test his technique on. Because rubidium has a very well understood energy level structure, it will be easier to show that the comb laser provides the expected increase in resolution. It may also be possible to distinguish small changes in the hyperfine structure of rubidium due to dipole-dipole interactions, which to our knowledge has not been observed previously.

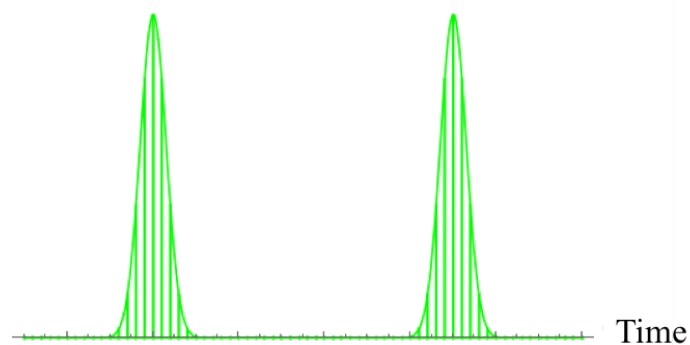


Fig. 4 – 2D with comb lasers. My work.

## **MOT Theory and Background**

### **1) History of the MOT**

The Magneto Optical Trap (MOT) is a device designed to produce samples of cold, trapped atoms in the millikelvin range. Dr. Steven Chu (at Stanford University), Dr. Claude Cohen-Tannoudji (at Ecole Normale), and Dr. William D. Phillips (at NIST, Maryland) each worked to develop the first MOT, with Dr. Chu's work focused largely on laser cooling, while Dr. Phillips developed magnetic trapping, and Dr. Cohen-Tannoudji pursued theoretical work on atomic cooling. Their work in the late 1980's and early 1990's eventually earned the trio the 1997 Nobel Prize in Physics [2]. At a basic level, a MOT works by first laser cooling atoms in a vapor before trapping them with a clever application of the Zeeman effect. Cold, dense samples are useful in AMO physics because of the reduced Doppler broadening of spectral lines due to thermal motion, as well as the relative strength of signals from such a sample. It is also possible to evaporatively cool such a sample in order to produce a Bose-Einstein condensate. Because my work had a focus on applications for rubidium 87, all examples will be worked out for that case.

### **2) Laser Cooling**

#### *2.1 The Optical Doppler Effect*

It is a well-known result of thermodynamics that the temperature of a gas is related to the average kinetic energy of the atoms making up that gas. We can therefore cool a sample of gas by slowing down the individual atoms in the sample. A MOT slows down atoms by exploiting the optical Doppler effect with a technique called laser cooling. In essence, moving atoms will experience a different frequency of light depending on their direction of motion. Particles moving toward a light source will "see" an increase in frequency (a "blue shift"), while particles moving away from that same source will "see" a decrease in frequency (a "red shift"). The equation relating the frequency experienced by the atom to the frequency in the lab frame is given by [3]

$$f_{obs} = \sqrt{\frac{(1 + \beta)}{(1 - \beta)}} f_{sce} \quad (1)$$

$$\beta = \frac{v}{c} \quad (2)$$

where  $f_{obs}$  is the frequency as seen by the moving atom,  $v$  is the relative velocity between the atom and the source,  $c$  is the speed of light, and  $f_{sce}$  is the frequency at the source in the lab frame. The one-dimensional case extends quite naturally to the three dimensional case where there are three mutually orthogonal laser beams, each of which cools in just one direction. A diagram of the laser cooling process is given in figure 5.

## 2.2 The Light Force

A photon carries momentum related to its wavenumber according to [3,4,5]

$$\vec{P} = \hbar\vec{k}, \quad (3)$$

Where  $\vec{k}$  is the wave vector. Conservation of momentum dictates that any time an atom absorbs a photon, it must carry away the photon's momentum. The Doppler effect and conservation of momentum combine to form a cooling scheme. First, we tune a laser (the "trapping laser") to the "red" (low frequency) side of an atomic transition and stabilize its frequency (I discuss how we do this in section 4.3). We then divide the beam into three standing waves, as shown in figure 6. As atoms move parallel to any of the beams, their motion blue shifts the laser light into atomic resonance. The atoms are then able to absorb laser photons and carry away their momentum. Finally, the atoms will decay back into their ground states, emitting photons in a random direction and generating secondary momentum kicks. Because the atoms experience preferential absorption, the average effect of many such interactions is to slow the atoms down. The motion of any atom can be decomposed into components parallel to each of the three standing waves, so that in the region where the three beams overlap, the atoms will be slowed in every direction and come to a (nearly) complete stop.

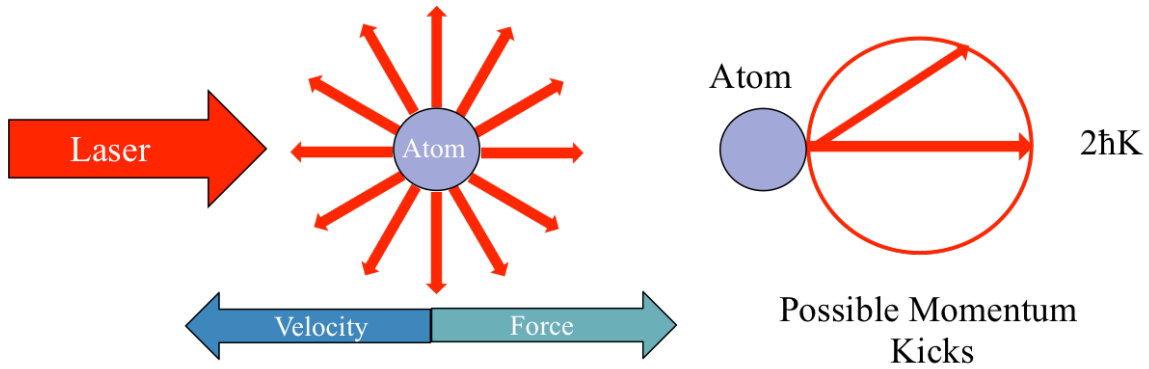


Fig. 5 - Demonstration of laser cooling. My work based on a figure in [4].

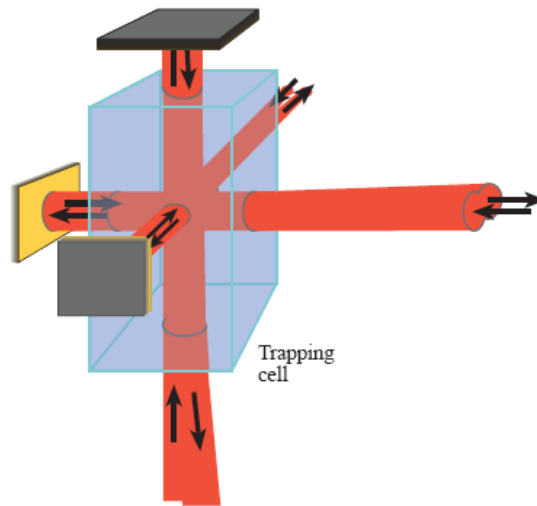


Fig. 6 - Arrangement of laser beams in a MOT. [4].

Each atom repeats this process many times in a very short period of time. We can therefore approximate the process as continuous, and talk about the concept of a “light force” [4]. The light force is not classical force, but rather an effective force describing a huge number of repeated interactions between the atoms in the sample and the laser. One equation for the light force is given by

$$\vec{F} = \hbar \vec{k} \frac{\Gamma}{2} \frac{\frac{I}{I_0}}{1 + \frac{I}{I_0} + \left( \frac{2\delta - \vec{k} \cdot \vec{v}}{\Gamma} \right)^2} \quad (4)$$

Where  $\vec{k}$  is the wave vector,  $I$  is the intensity of the laser,  $\Gamma$  is the decay rate of the atom's excited state,  $\delta$  is the frequency difference between the laser and the atomic transition,  $\vec{v}$  is the velocity vector of the atom, and  $I_0$  is the saturation intensity of the atoms [4]. This force has a maximum when intensity is allowed to increase to infinity given by

$$\vec{F}_{max} = \hbar \vec{k} \frac{\Gamma}{2} \quad (5)$$

So the force is limited by the decay rate of the excited state (atoms in the excited state are inaccessible to the laser, so their momentum is a constant until they decay). To get an estimate for the size of this force (and the relevant time scales within a MOT), I've calculated the force acting on a Rb 87 atom at room temperature ( $\sim 298$  K). The parameters are [4]

$$\begin{aligned} \Gamma &= 3.77 * 10^{-7} \text{ Hz}, & |\vec{k}| &= 8.055 * 10^6 \text{ m}^{-1}, & |\vec{v}| &= 269.298 \text{ m/s}, \\ I_0 &= 1.6 \text{ mW/cm}^2, \\ m &= 1.4432 * 10^{-25} \text{ kg}, & I &= 40 \text{ mW/cm}^2, & \delta &= 10 \text{ MHz} \end{aligned}$$

Which gives an acceleration of  $1.07 * 10^{11} \text{ m/s}^2$  (assuming the wave vector and velocity vector to be antiparallel). A similar calculation is undertaken in [4] for Rb 85 atoms, gives  $1.1 * 10^{11} \text{ m/s}^2$ , so the value I obtained is not as extreme as it might at first appear. Atoms in a MOT are therefore cooled nearly instantaneously (since this accelerator is antiparallel to an atom's velocity). Once the atoms are cooled, the Doppler effect drops them out of resonance; so cooled atoms will not encounter the light force and will never turn around. This assumes that there are not so many atoms that the thermal motion of nearby atoms knocks cooled atoms out of the trap, so it is important to keep the pressure within a MOT low to reduce the number of collisions.

### 2.3 Dark State Transitions and the Repump Laser

We have so far treated atoms as two level systems with only ground and excited states available. While this simplifies the analysis, it leaves out important physics, in particular the so-called "dark state" transitions that often exist around the cooling transition. Figure 7 shows the dark state transitions in the energy level diagram for Rb 87.

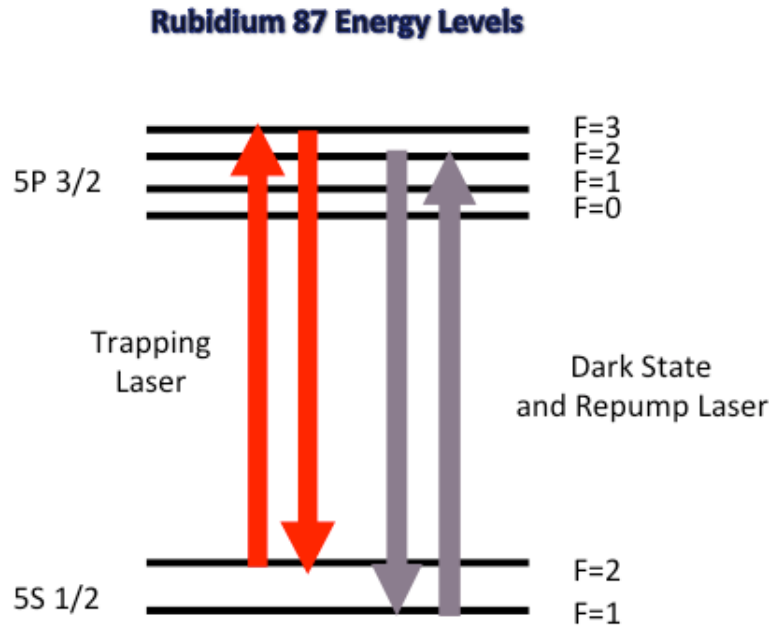


Fig. 7 - Dark State transitions for Rb 87. Diagram is my own work based on [6].

In figure 7, the trapping laser is red detuned from the  $5S_{1/2} (F = 2) \rightarrow 5P_{3/2} (F' = 3)$  cooling transition ( $\approx 780 \text{ nm}$ ). However, it is also possible to, with low probability, excite the  $5S_{1/2} (F = 2)$  to  $5P_{3/2} (F' = 2)$  transition. From the  $5P_{3/2} (F' = 2)$  state, the atom can then decay into the  $5S_{1/2} (F = 2)$  or  $5S_{1/2} (F = 1)$  state. If it decays into the  $5S_{1/2} (F = 1)$  state, the atom will become inaccessible to the trapping laser, and it will fall out of the cooling cycle. MOTs combat dark state transitions with a second laser, the so-called “repump” laser. We tune our repump laser to the  $5S_{1/2} (F = 1)$  to  $5P_{3/2} (F' = 2)$  transition to force atoms out of the dark states and back into the cooling cycle [6]. As with the trapping laser, we actively stabilize the frequency of the repump to ensure the continuous operation of the MOT.

### 3) Magnetic Trapping and the Zeeman Effect

MOTs are designed to spatially trap atoms in addition to cooling them down. To do so requires us to generate a force analogous to the spring force, which has the effect of drawing atoms into the center of the trap. How we go about producing this force is complex. Rb 87 atoms in our trap are neutral and have very low mass, so none of the

fundamental forces are very useful. However, it is possible for us to exploit the Zeeman effect in order to create a second effective force with the properties we require.

### 3.1 The Zeeman Effect

The Zeeman effect is the splitting of degenerate energy levels into a non-degenerate configuration in response to an applied magnetic field [7,8,9]. The excited state of the transition used for cooling is, in most cases, degenerate and subject to the Zeeman effect. If we arrange for a magnetic field in the MOT chamber to have a constant gradient away from the intersection of our lasers, we shift the energy levels of atoms not in the center of the trap into resonance with the trapping laser so that momentum kicks (as described in section 2.2) push them into the center of the trap in addition to cooling them. This is illustrated diagrammatically in one dimension for a rubidium atom in figures 8 and 9.

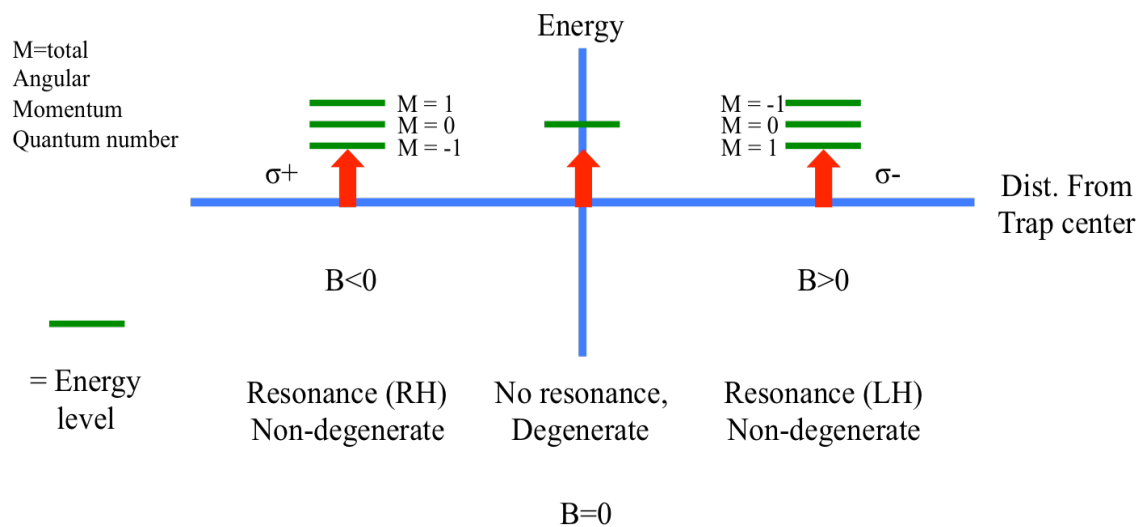


Fig. 8 - The Zeeman effect for trapping. My work based on a figure in [4].

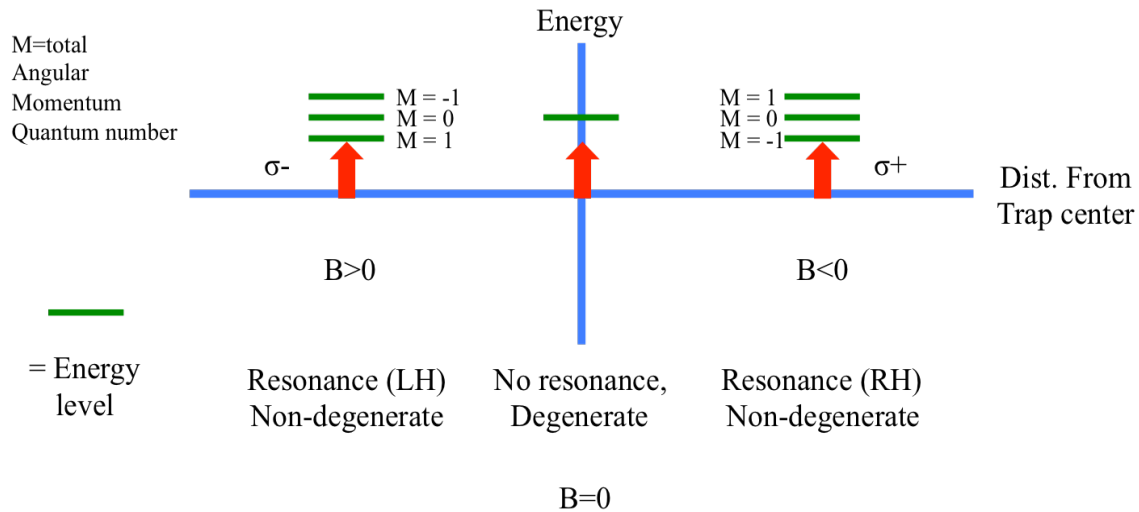


Fig. 9 - Alternate trap configuration. My work based on a figure in [4].

These figures illustrate the one-dimensional case, but the three dimensional case is a simple extension of the principle. We generate our magnetic field with a pair of anti-Helmholtz coils with the trap at their center. Figure 10 shows the anti-Helmholtz coils around a MOT.

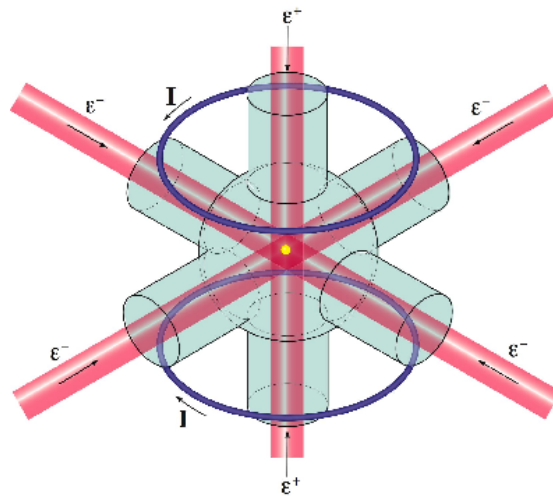


Fig. 10 - Full MOT configuration.  $\vec{I}$  indicates the direction of the current through the coils, and the yellow spot marks the location of the trap. [9].

Without cooling lasers, an atom would naturally oscillate between two turning points on either side of the trap. The cooling lasers serve to damp this oscillation so that the atom will eventually settle into the center of the trap and remain there until disturbed. For this reason, it is common to refer to the region in which all three standing waves overlap and

an “optical molasses”. Functionally, the total force on an atom within a MOT would take (approximately) the form

$$\vec{F} = -k\vec{x} - \beta\vec{v} \quad (6)$$

Where  $\vec{x}$  is the position vector of the atom relative to the center of the trap and  $\vec{v}$  is its velocity in the same coordinate system, with  $k$  and  $\beta$  constants. The important thing to note here is the functional form, which is identical to a spring with air resistance included.

### 3.2 Polarization States

Figures 6,7, and 8 label the incoming laser beams with polarization states (RH or  $\sigma +$  for right handed circularly polarized light, LH or  $\sigma -$  for left handed circularly polarized light). This is a critical point; selection rules only allow the trapping transitions to occur for circularly polarized light of the correct handedness. This is opposed to our laser cooling process, which does not require any particular polarization. Selection rules are covered more thoroughly in [5,7]. However, the light generated by our lasers is linearly polarized. We convert the laser to circular polarization with quarter-wave plates, which use a birefringent material to delay part of an electromagnetic wave. This delay is the cause of the conversion of linear light into circular light (or elliptical light if the wave plate is not properly oriented). There are also half-wave plates, which rotate linearly polarized light but maintain a linear polarization. They differ from half waveplates only in the amount of delay introduced, and are discussed more in later sections. Waveplates are covered very thoroughly in [5]. In summary, a MOT work as follows: we set a trapping laser to the red side of some atomic transition that we use for cooling. We then merge a secondary repump laser (designed to account for the dark state transitions) with the trapping laser, and divide the combined beam into three parts. We circularly polarize the beams with quarter wave plates (to the appropriate handedness) and pass them through the sample at 90-degree angles to each other, all overlapping at one point. We then reflect the beams back through the chamber to form standing waves, and pass them through secondary quarter-wave plates between the mirror and the chamber to return them to the correct handedness (reflection flips the handedness of circularly polarized light [5]). We arrange anti-Helmholtz coils around the chamber to produce a magnetic

field gradient outward from the intersection of the three beams, and the MOT is complete. The trap will begin to fill with atoms according to

$$N(t) = N_0 \left(1 - e^{-t/\tau}\right) \quad (7)$$

$$1/\tau = n\sigma v \quad (8)$$

$$N_0 = \left(\frac{0.1A}{\sigma}\right) \left(\frac{v_{max}}{v}\right)^4 \quad (9)$$

where  $N$  is the number of atoms in the trap,  $\sigma$  is the cross section of those atoms,  $v$  is their average velocity when the trap is turned on,  $v_{max}$  is their maximum velocity when the trap is turned on, and  $A$  is the surface area of the trapping region [8].  $N_0$  is the upper limit of the trap and is determined by the collision parameters of the atoms.

#### 4) External Cavity Diode Lasers (ECDLs)

External cavity diode lasers provide us with two key advantages over other common lasers (i.e. Ti Sapphire lasers, HeNe lasers, etc.). Firstly, ECDLs have a high degree of tunability. This means that we can control the frequency of the laser over a large range, which allows us to conduct spectroscopy experiments that help us to stabilize our lasers. ECDLs are also relatively cheap and easy to both build and repair, which makes them ideal for an undergraduate experiment. This section will outline how ECDLs in general work and steps we've taken to improve our own lasers.

##### 4.1) Basic Picture

In an external cavity diode laser, light is initially generated by a laser diode. Because the front and back surfaces of a laser diode are partially reflective, the light must form standing waves subject to boundary conditions set by the size of the diode. This results in a bare diode generating many longitudinal modes, all with wavelengths that are 1 over some integer fractions of the largest possible wavelength [5,10]. The strength of each mode is dictated by the properties of the gain medium within the diode and environmental factors such as temperature. Ideally, we would like to select a single mode for our laser to operate in, which we can do with the cavity of an ECDL. In its most basic form, an ECDL couples a laser diode to a cavity in order to provide optical feedback to the diode. This feedback suppresses most of the modes emitted by a bare diode, resulting in single mode operation of the laser. It is then possible for us to control

the frequency of the laser by manipulating parameters of the cavity (primarily the orientation of a diffraction grating within the cavity), giving the laser a high degree of tunability. The relevant equation is [3,5,10]

$$n\lambda = 2d\sin(\theta) \quad (10)$$

Where  $n$  is the “order” of the diffracted beam,  $\lambda$  is the wavelength of the diffracted beam,  $d$  is the separation of ridges on the diffraction grating, and  $\theta$  is the angle the incident beam makes to the surface normal of the diffraction grating. This equation describes how light is dispersed by a diffraction grating. In an ECDL, the first order diffracted beam is retroreflected back into the laser diode as the source of optical feedback. So by setting  $n = 1$  in equation 9 and knowing the ridge spacing of the diffraction grating used in our laser, we are able to set the wavelength of our laser by controlling  $\theta$ . The mechanism used to control the grating angle is discussed in section 5 of my thesis. This tunability is critical for the successful operation of a MOT, which is highly sensitive to the frequency of the trapping and repump lasers. There are two common approaches to the cavity configuration, namely the Littman-Metcalf configuration and the Littrow configuration. For my experiment, we exclusively used the Littrow configuration.

#### *4.2) Littrow Configuration*

The Littrow configuration couples the first order diffracted beam directly into the laser diode from the diffraction grating, with the zero order beam (which undergoes ordinary reflection) exiting as the primary beam going to the experiment. This configuration has the advantage of being relatively simple, but doesn't work well at wavelengths with very large or very small diffraction angles. In addition, when the diffraction grating is adjusted, it also changes the path of the zero order beam. So if whenever we adjust the grating, we misalign the experiment slightly. The setup is shown diagrammatically in figure 11.

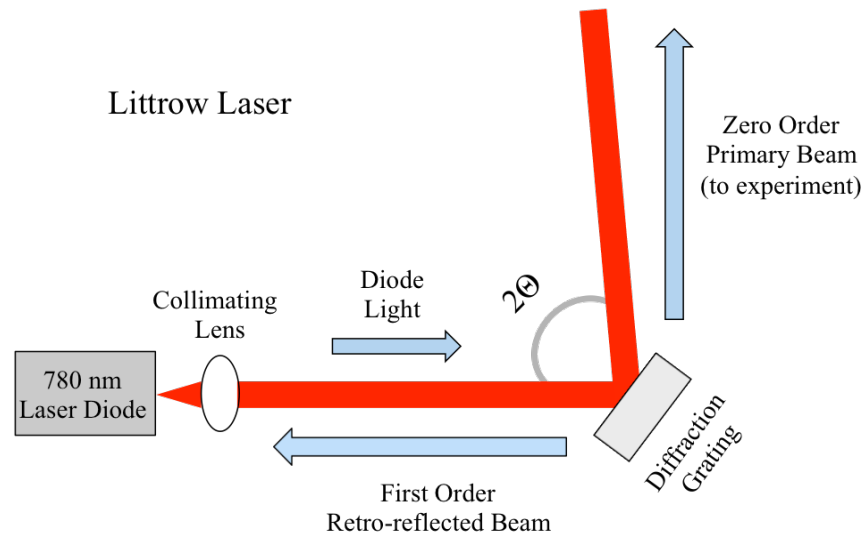


Fig. 11 - Littrow laser diagram. My work.

Despite the control the grating provides us, a Littrow laser is still subject to frequency drifts due to changes in temperature and mechanical vibrations. We account for these drifts by actively stabilizing the laser's frequency.

#### 4.3) Frequency Stabilization and Saturated Absorption Spectroscopy

It is common to determine the frequency of lasers used for optical trapping by employing a technique known as Doppler-free saturated absorption spectroscopy. The technique is shown diagrammatically in figure 12.

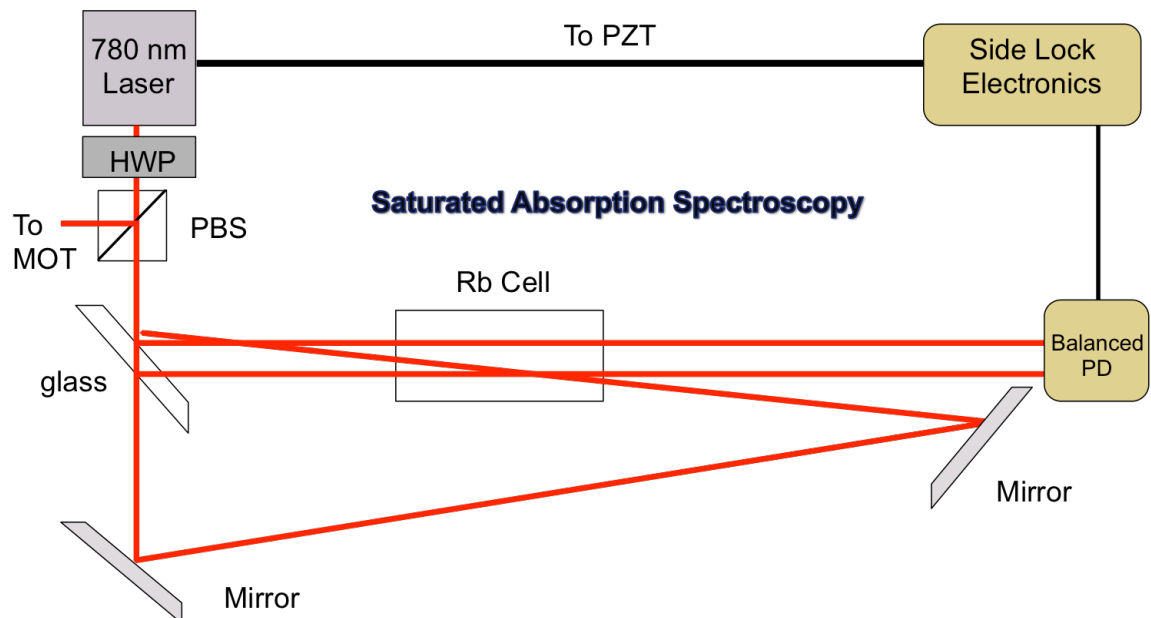


Fig. 12 - Saturated Absorption Spectroscopy. My work. HWP is a half-wave plate, and PBS stands for polarizing beam splitter.

The primary beam exits the laser and passes through a half-wave plate (HWP). A half-wave plate is a thin sheet of birefringent material that changes the polarization of any linearly polarized light that passes through it. We then use a polarizing beam splitter (PBS) to separate the beam into two components, with one component going on to the MOT and the other conducting the saturated absorption spectroscopy. The half-wave plate allows us to send the majority of the beam into the MOT while sending a very small amount into the spectroscopy setup. We split the weaker beam into three components with a thin piece of glass – two probe beams (reflections off of the front and back surfaces of the glass) and a pump beam (the transmitted portion of the beam). We then send the two probe beams through a cell filled with rubidium vapor and into a balanced photodetector. This allows us to measure the transmission/absorption of the two probe beams relative to each other. We reflect the pump beam through the cell from the far side; counter propagating it against one of the probe beams. To obtain a signal containing the relevant hyperfine structure of the sample, we vary the wavelength of the laser by applying an AC voltage across a piezoelectric transducer (pzt) mounted behind the diffraction grating within our laser. This causes the grating angle to vary in time, which in turn scans the wavelength of the laser according to equation 9. As we scan the wavelength of the laser, we pass over atomic resonances. For the probe beam that doesn't encounter the pump, this produces a Doppler broadened spectrum, as shown below in figure 13.

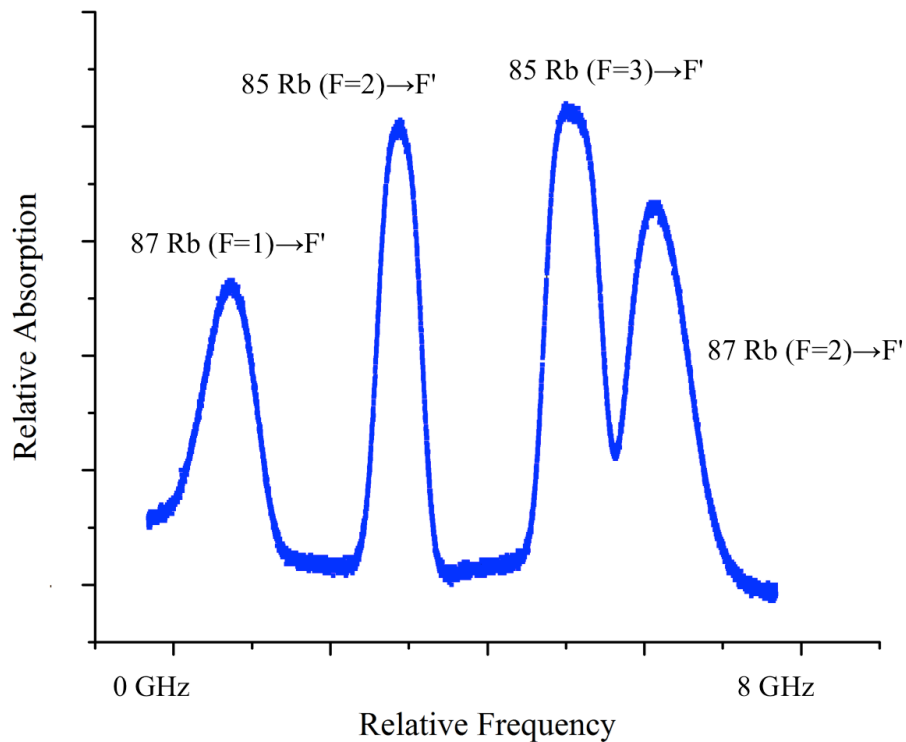


Fig. 13 - Doppler Broadened Spectrum of Rb. Generated from my oscilloscope (arbitrary units, frequency range is  $\sim 8$  GHz).

Note that these peaks are a measure of absorption, while an inverted signal would be a measure of transmission. When the laser's frequency is close to an atomic resonance, moving atoms will see the frequency of the laser blue-shifted into resonance and will absorb a photon. Assuming a standard Maxwellian distribution of the velocities of the atoms, this means that as the laser gets closer to atomic resonance, it will be more strongly absorbed by the sample because there are more atoms at zero velocity (where there is no Doppler shift) than at any other velocity. It is the optical Doppler effect, which causes the peaks here to be so broad. The second probe beam encounters the pump, and we obtain a spectrum like figure 14.

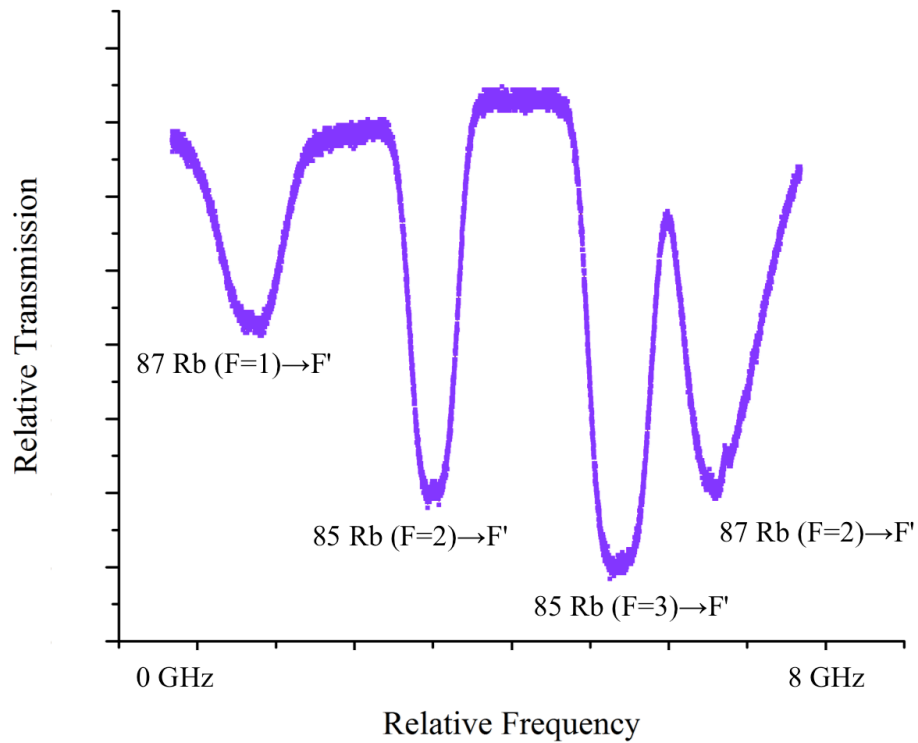


Fig. 14 - Doppler Broadened Peaks and Hyperfine Structure. Generated from my oscilloscope (arbitrary units, frequency range is ~8 GHz).

Note that these peaks measure transmission – they are inverted relative to figure 13 in order to obtain the difference between the two signals. This spectrum shows both Doppler broadened peaks and the smaller hyperfine structure of the individual transitions. Because the probe beam and the pump beam are propagating in opposite directions to one another, they will typically interact with different groups of atoms on either side of the velocity distribution, as shown in figure 15.

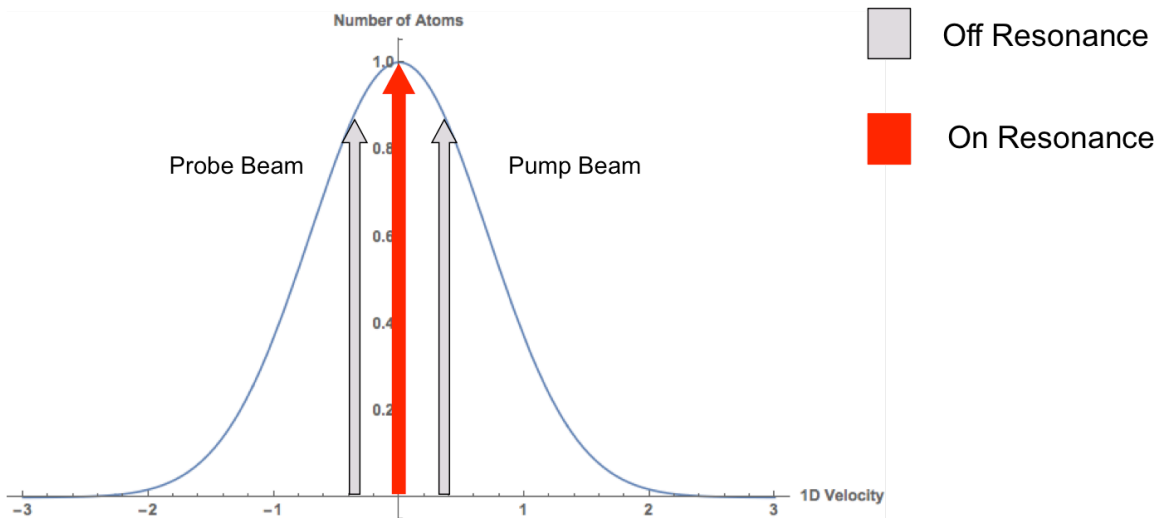


Fig. 15 - A typical Maxwellian velocity distribution. The arrows indicate which atoms will be resonant with which laser. My work.

So, while the laser is off resonance our scan produces ordinary Doppler broadened peaks, because the two beams are interacting with different groups of atoms and don't effect one another. However, when the laser is exactly on an atomic resonance (that is, a hyperfine line), they both interact with the same group of atoms – those with zero velocity. Since the pump beam is much more intense than the probe beam, it excites nearly all of the stationary atoms. This leaves no atoms left to absorb the probe beam, so nearly the entire beam is transmitted. This effect is sometimes referred to as “spectral hole burning”, and when the laser is exactly on resonance it produces our hyperfine lines. Our photodetector adds the pure Doppler broadened spectrum to the inverted Doppler + hyperfine spectrum to produce a pure hyperfine signal, as shown in figure 16.

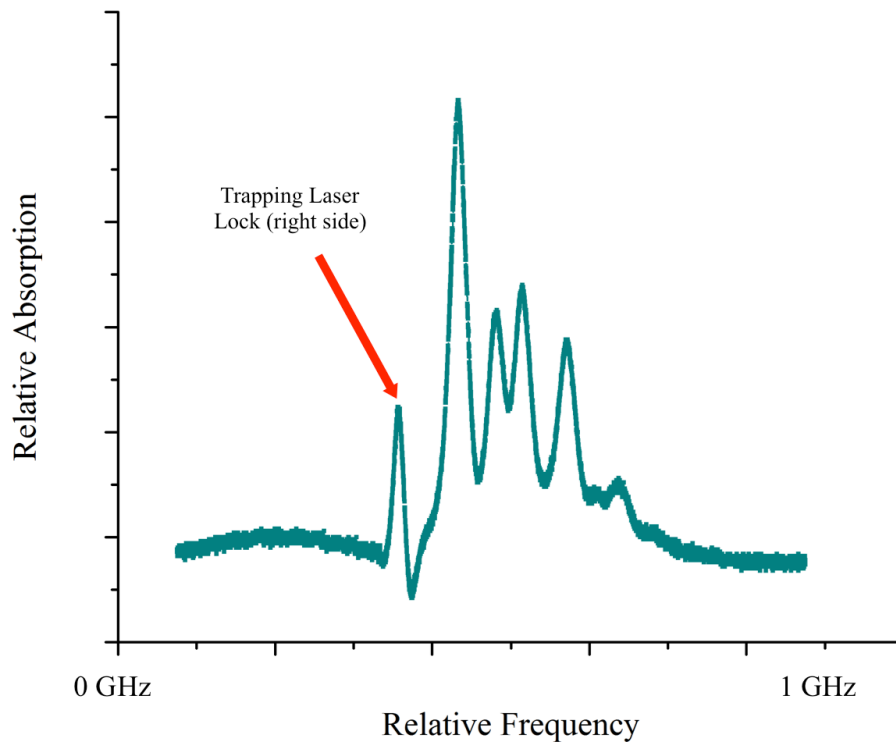


Fig. 16 - Pure hyperfine signal ( $5S_{1/2} F = 2 \rightarrow 5P_{3/2} F'$ ). Generated from my oscilloscope (arbitrary units, frequency range is  $\sim 1$  GHz).

The next step toward stabilizing the frequency of our lasers is to select the hyperfine peak we use for cooling/repumping in the MOT. In the case of the trapping laser, we use the  $5S_{1/2} F = 2 \rightarrow 5P_{3/2} F' = 3$  transition. To select this transition, we slowly decrease the amplitude of our AC signal to the PZT (called the ramp signal), while adjusting the DC offset to that signal (called the bias). This enables us to conduct the scan in a narrow region around the peak of interest, producing a signal like figure 17.

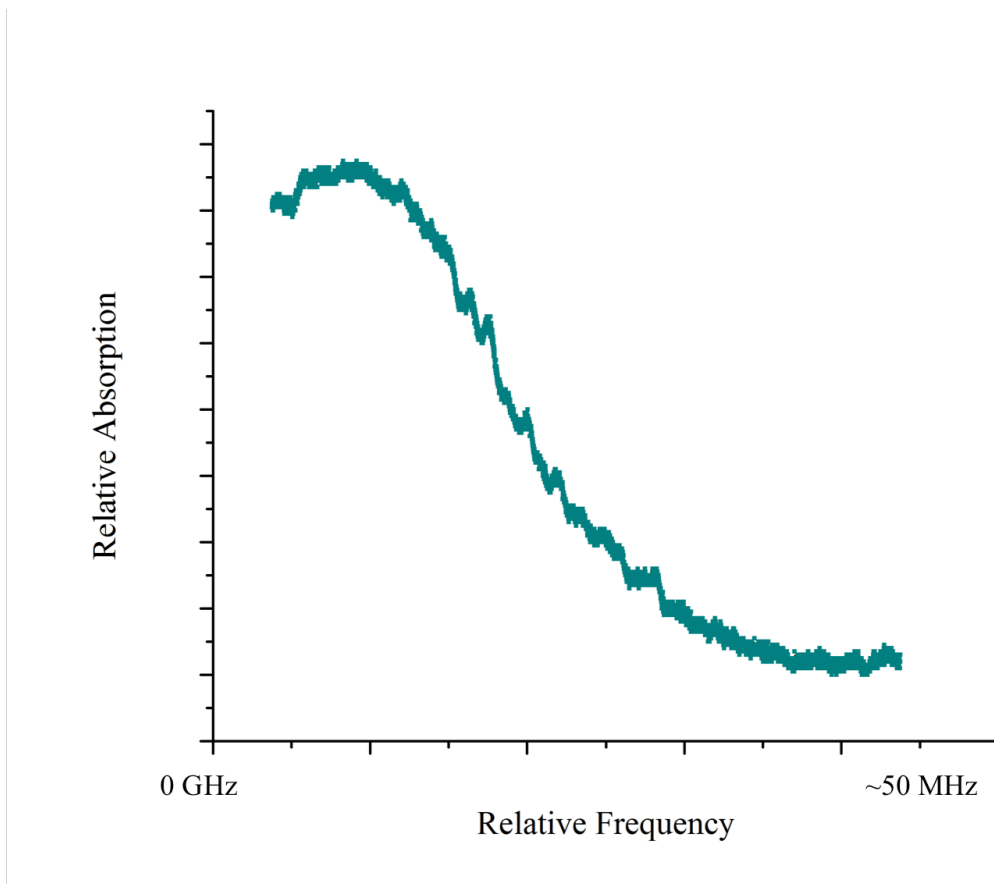


Fig. 17 - Zoomed in signal. Generated from my oscilloscope (arbitrary units, frequency range is  $\sim 50$  MHz).

We then add a DC offset to the signal and feed it into sidelocking electronics. The sidelock electronics generate an error signal based on the offset of any signal it receives from zero volts. We add the DC offset to our photodetector signal to control which part of the peak is at zero volts, which in turn controls the frequency our electronics will lock to. Our electronics allow us to stabilize the frequency of our laser to within  $\sim 10$  MHz for periods of several hours. Similar schemes are discussed in greater detail in [10,11,12,13] for the interested reader. This scheme is ideal for the trapping laser, which needs to be red detuned from atomic resonance to cool effectively. The repump laser however needs to excite atoms that are already at least partly cooled, so we must set it to a resonance peak. Rather than use a more involved peak locking scheme, we simply sidelock the repump laser and then shift it into resonance with an acousto-optic modulator. The details of an acousto-optic modulator are beyond the scope of my work, but they are able to shift the

frequency of light by a set amount. The specifics regarding our repump laser are discussed further in section 5.2.

#### *4.4) Mode Hopping*

Previous sections have neglected other factors that often become important when operating an ECDL in a lab setting. The factor of greatest importance in the lab is mode hopping. It is possible for an ECDL to transition into a different mode of operation due to a number of factors, including temperature drifts within the laser diode itself, and mechanical noise within the cavity. We suppress mode hopping in three ways. First, we control the temperature with a JILA laser diode temperature controller. The controller works by reading the temperature of the diode with a thermistor mounted near the diode. The resistance of a thermistor is a function of temperature, so the controller is able to convert a measurement of resistance into temperature. It then generates an error signal, which it sends to a thermoelectric cooler (TEC). Applying a voltage across a TEC generates a temperature difference across the TEC via the Peltier effect, which in turn allows us to set the temperature of the diode. Diode temperature also has a role in determining the wavelength of maximum gain for the diode. What that meant for us practically is that once our ECDL cavity was aligned, we could adjust the temperature of the diode until the output power reached a maximum. The JILA controller stabilizes the temperature of the diode at the value we selected, maintaining maximum output power while suppressing any temperature related mode hopping. Our system is stable to within a tenth of a degree Celsius, and shows no long-term drifts. Our second method for controlling mode hops is a Faraday isolator, which prevents back reflections from the experiment into the laser cavity. The isolator rotates the polarization of any beam that passes through it by  $45^\circ$  regardless of which direction the beam is propagating. The beam initially passes through a rotated PBS so that all the light from the laser enters the Faraday isolator. The isolator then rotates the beam by  $45^\circ$ , and it passes through a second PBS which is rotated  $45^\circ$  relative to the first PBS. So once again, the PBS transmits all the light from the laser. Any back reflection passes through the second PBS normally on its way back to the laser cavity. The isolator rotates it by an additional  $45^\circ$ , so that the back reflected beam is now polarized at  $90^\circ$  relative to the initial beam. It is

therefore entirely reflected by the first PBS and cannot reach the laser cavity. I've drawn a schematic for this setup in figure 18.

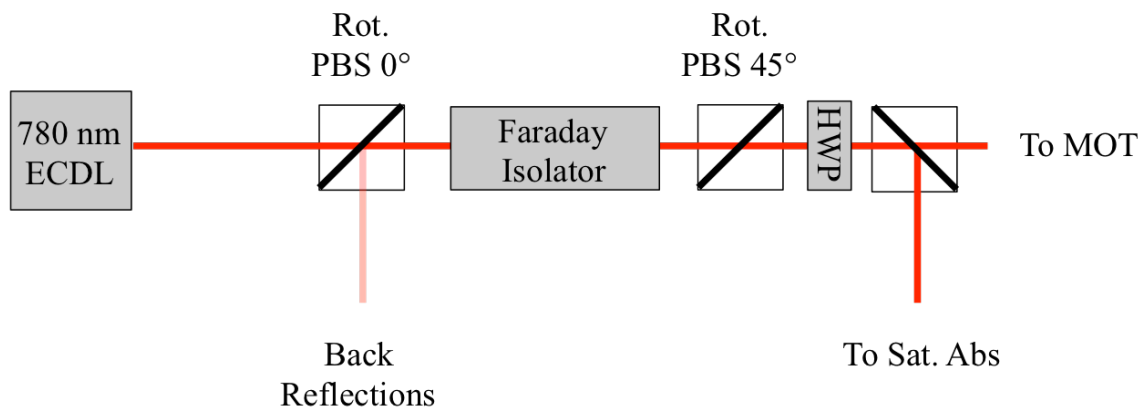


Fig.18 - Faraday Isolator. My work. HWP is a half-wave plate, and Rot. PBS stands for rotated polarizing beam splitter.

Finally, we suppress mode hopping during a frequency scan of the laser with a technique we refer to as feed forward. We scan the laser diode current simultaneously with the diffraction grating pzt so that the gain profile of the diode shifts to match the wavelength we are selecting for. This allows us to scan across the entire 8 GHz Doppler broadened spectrum of our sample mode hop free. For this technique to work properly, we had to determine what effect a change in current had on the output frequency of the diode. We removed the diffraction grating from our ECDL cavity and replaced it temporarily with a mirror, so that we could see the effects on the bare diode with no feedback. We then read the wavelength of the laser light with a wave meter as we scanned the diode current. Plots of the three data sets we obtained for the trapping laser diode are given in figures 19-21.

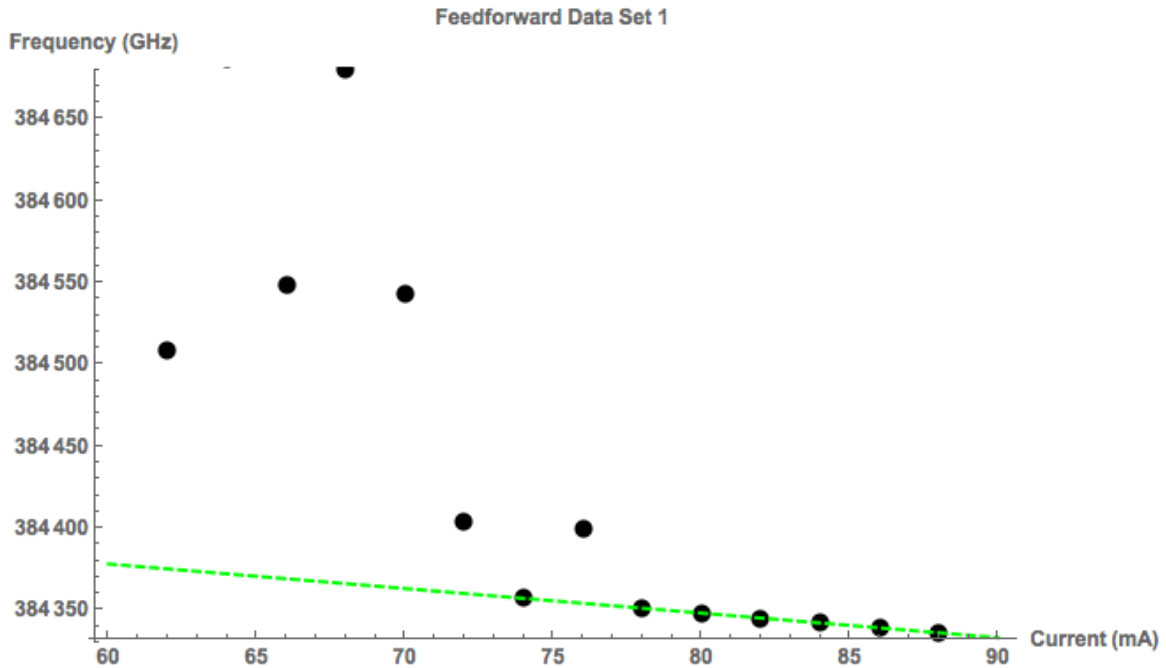


Fig. 19 – Feed forward data set 1. Mathematica plot generated from my data. The best-fit line to the mode hop free data has a slope of  $-1.5 \text{ GHz}/\text{mA}$ .

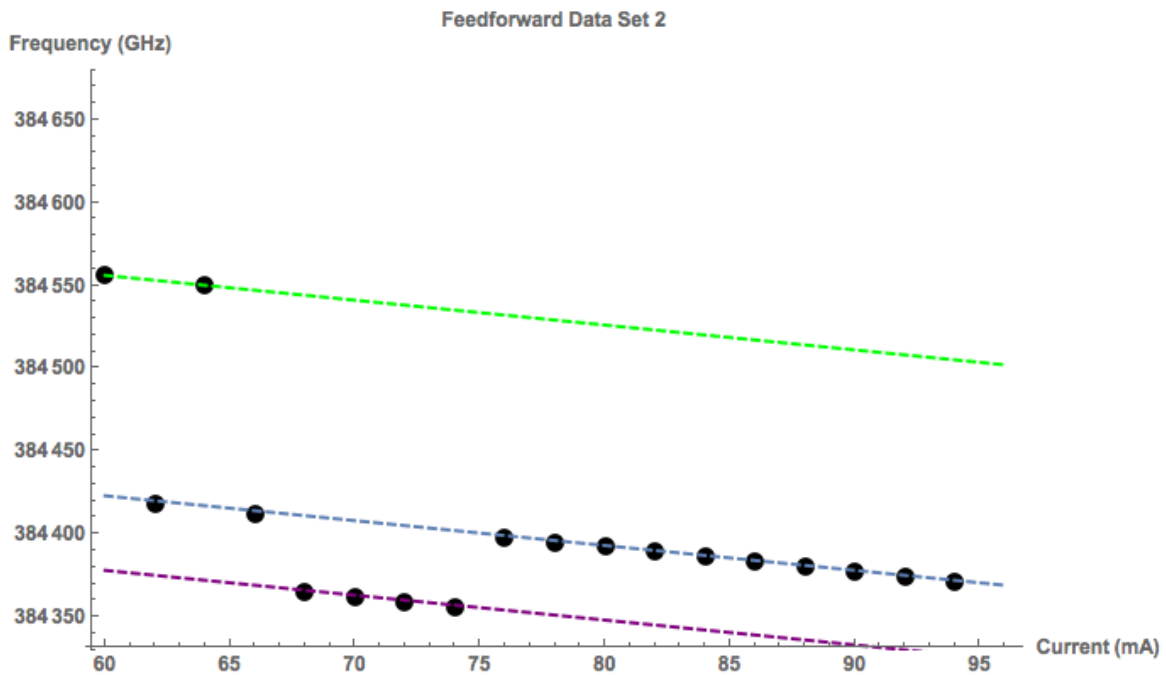


Fig. 20 – Feed forward data set 2. Mathematica plot generated from my data. Each line has a slope of  $-1.5 \text{ GHz}/\text{mA}$  and represents a different laser mode.

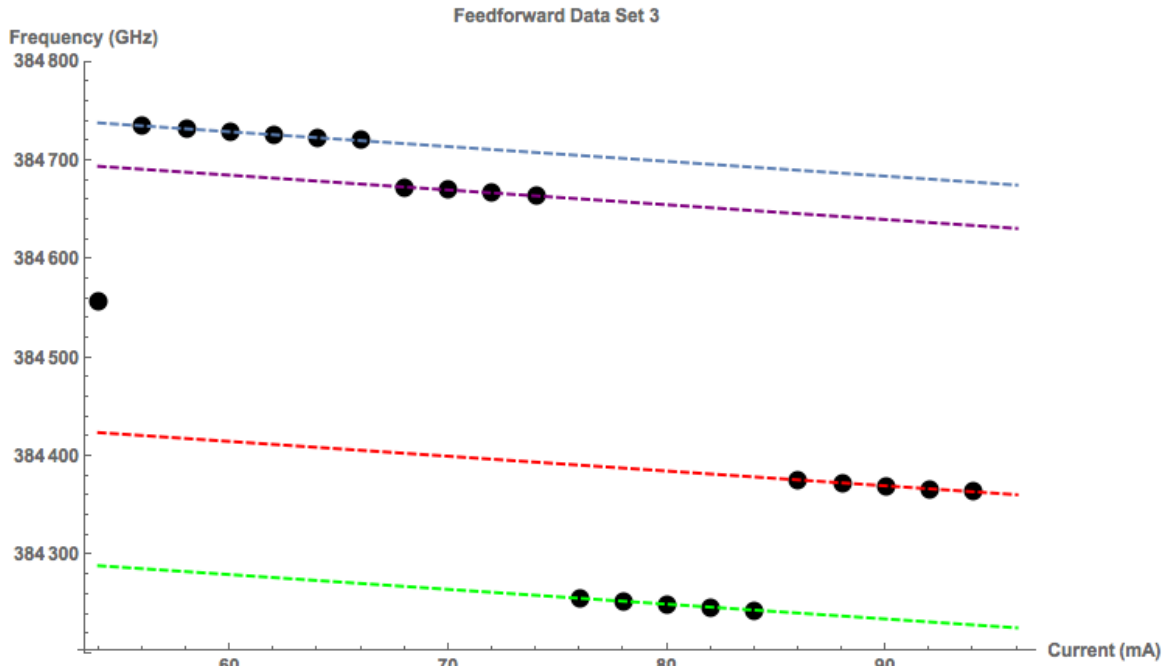


Fig. 21 – Feed forward data set 3. Mathematica plot generated from my data. Each line has a slope of  $-1.5 \text{ GHz}/\text{mA}$  and represents a different laser mode.

The dashed lines in each plot represent different modes of the laser. Within a given mode, we found that  $\frac{df}{dI} = -1.5 \frac{\text{GHz}}{\text{mA}}$  where  $f$  is the frequency of the laser and  $I$  is the diode current. Jumps between the different lines in the data are mode hops that occurred during our scan. With this figure we were able to determine that we needed to reduce the amplitude of the pzt ramp signal before using it to scan the current. We built a simple potentiometer circuit so that we could vary the attenuation of the ramp by hand, and were able to adjust it until we achieved a mode hop free scan of the rubidium spectrum. We then copied the circuit and followed the same procedure for the repump laser with the same success. Mode hopping and the suppression of mode hopping are discussed very thoroughly in [10] for the interested reader.

## **MOT Construction and Characterization**

### **5) Construction and Characterization of the ECDLs**

The bulk of my time on this project was spent building and aligning the lasers. When I began the project, we had a commercial laser, which was ultimately too weak for our

purposes, so it was deemed necessary to construct out own. The cavities are a JILA machine shop design with built in temperature controls in the form of a thermoelectric cooler (TEC) mounted below the laser diode. Each laser has the same cavity configuration and diffraction grating, but different diodes and current/temperature settings.

### 5.1) *The Trapping Laser*

Figure 22 is a picture of the trapping laser I built with labels to indicate the various components of the system. The diode is a Sanyo DL-7140201w, which operates at 71.5 mA and 21.8°C. The laser produces 27 mW of power, of which ~1 mW is used for saturated absorption spectroscopy and side locking, while ~23 mW are sent to the MOT (~3 mW is lost to the Faraday isolator).

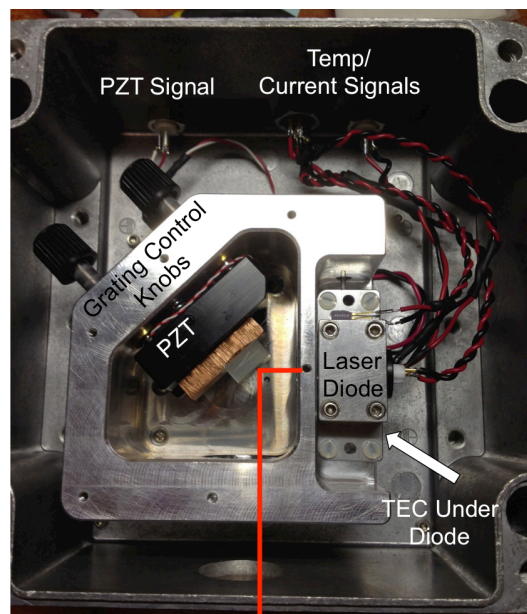


Fig. 22 - My trapping laser. Repump laser is the same basic setup.

The laser has been through several iterations due to part failure on a number of occasions, as well as modifications we have made to optimize the laser's performance. I inserted a copper plate between the diffraction grating and the standard grating mount to increase the separation between laser modes (also called the "free spectral range") and had the front window of the laser cavity anti-reflection coated after we had issues with secondary feedback. I made similar modifications to the repump laser.

### 5.2) *The Repump Laser*

Our repump laser was built in the same configuration as our trapping laser. The diode is a Sharp LT024MF0, which operates at 60 mA of current and 21.2°C. It also uses a feed forward system to control mode hopping. We lock the repump laser to the side of a crossover peak in the  $5S_{1/2} F = 1 \rightarrow 5P_{3/2} F'$  hyperfine transitions and shift it by 80 MHz with an AOM to the  $5S_{1/2} F = 1 \rightarrow 5P_{3/2} F' = 1$  transition in order to maintain a closed optical loop for our cooling cycle. It outputs 60.4 mW of power, of which 3 mW is used for spectroscopy and frequency locking. The remainder goes into the MOT chamber along with the trapping beam. We didn't use a Faraday isolator with the repump laser because the AOM is effective at limiting back reflections from our experiment. We use a somewhat involved scheme to overlap the trapping and repump lasers and align them into the MOT, which is discussed in section 5.3.

### 5.3) *Configuration of the Laser Into the MOT*

Getting both lasers into the MOT with the correct polarization states was a challenge. We first needed to overlap the trapping and repump lasers to create a single beam. We did so by using half waveplates to set the polarization of the two lasers at 90° relative to one another, with the trapping laser P polarized and the repump laser S polarized. We then merged the beams with a polarizing beam splitter. We also expanded the beam in order to maximize the size of our cooling region. In our case, we expanded the beam from ~ 3mm diameter to ~ 9mm diameter, so that it would still be able to pass through our 1 cm diameter waveplates. We expanded the beams with two lenses of different focal lengths. The first has a focal length of 5 cm, and the second has a focal length of 15 cm. I put the 3 mm diameter beam through the 5 cm lens first. There is then a 20 cm space between the 5 cm lens and the 15cm lens. The beam reaches its focus at the 5 cm mark, and then diverges for the remaining 15cm, reaching 9 mm in diameter by the 20 cm mark. The 15 cm lens then collimates the light to maintain the 9 mm diameter of the beam. Next, we divided the beam into three parts. It is important that each beam have an equal amount of trapping power; so we arranged each beam to have a third of the total power of the trapping laser with the repump laser blocked. We did so by setting the polarization of the trapping laser with a half-wave plate such that a third of the power is transmitted through

a PBS while two thirds are reflected into a non-polarizing beam splitter. The non-PBS then divides the reflected beam into equal parts since it is not polarization dependent. There are then two S polarized beams and one P polarized beam. We require two right-handed beams and one left-handed beam (or vice versa) for the MOT, so we set all the quarter-wave plates at the same angle. Because of the experimental difficulty associated with determining the handedness of circularly polarized light, we found that it was simpler to orient the waveplates at  $-45^\circ$  and simply flip the direction of the magnetic field in the MOT (by running our anti-Helmholtz coil current backwards) if the handedness was wrong. The repump laser is unevenly divided and has opposite polarization to the trapping laser; repump power and polarization are not critical. Our scheme is fully drawn out in figure 23.

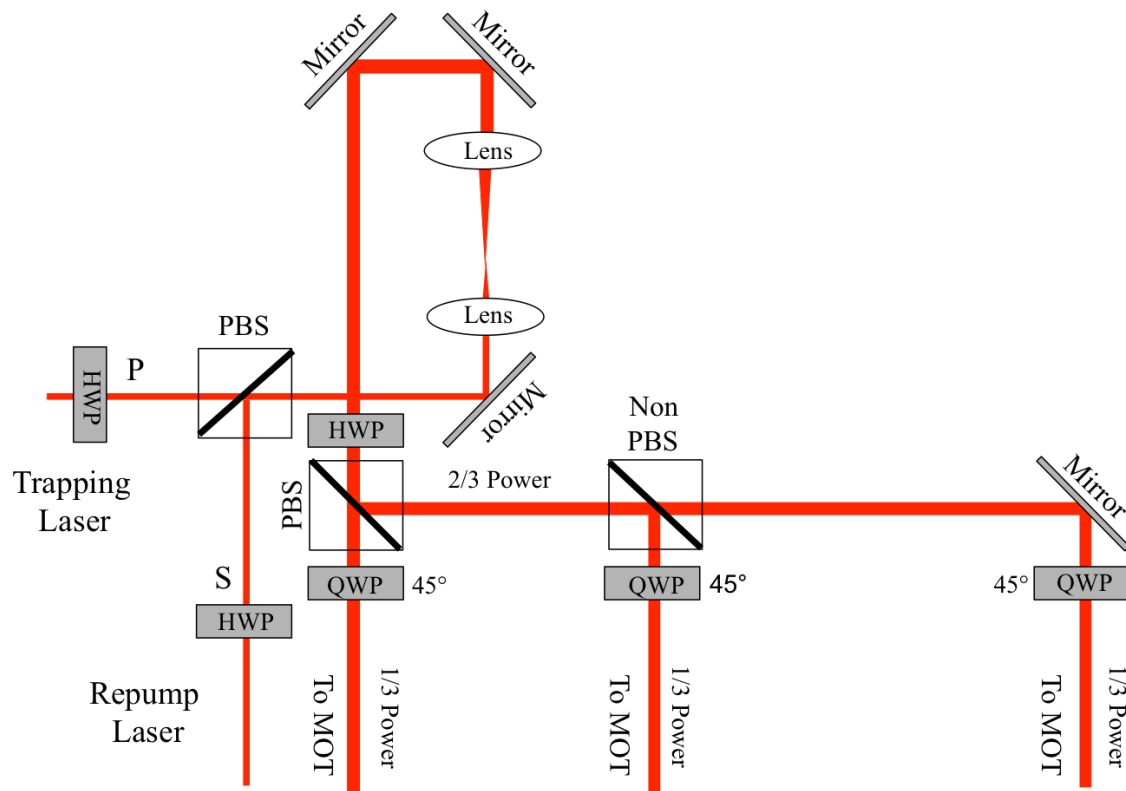


Fig. 23 - Arrangement of the laser into the MOT. My work. HWP is a half-wave plate, QWP is a quarter-wave plate, and PBS stands for polarizing beam splitter.

#### 5.4) The MOT Chamber

The MOT chamber itself is glass connected to an ion pump and surrounded by copper anti-Helmholtz coils used to generate the magnetic field for trapping. It is the same

chamber used by Dr. Adela Marian in [6]. The pump allows us to empty the chamber of air and refill it with a dilute rubidium vapor, which we generate with one of four “getters” within the chamber. The getters are strips of rubidium salt that release rubidium vapor when a current passes through them. We run ours at 2.4 Amps, which we found allows the chamber to maintain an equilibrium pressure on the order of  $10^{-9}$  Torr. We run the coils at 4.5 Amps, which produces a magnetic field gradient of 10 G/cm [6]. As of the time of this writing, the MOT is not operational. We are unsure what the problem is, but we are investigating and will hopefully get the system working in the near future.

### **Conclusions and Future Work**

In this thesis, I have endeavored to construct a magneto optical trap for rubidium 87 atoms. While the MOT is not yet working, I have made a great deal of progress toward its completion by building and characterizing two external cavity diode lasers, constructing and modifying electronics, and setting up the experimental apparatus. I have also spent some time attempting to debug the system, and have ruled out several possible issues including incorrect polarization and pressure issues within the MOT chamber. In the course of my thesis defense, it occurred to Dr. Jun Ye that we may have been setting our lasers too close to atomic resonance (i.e. we do not have a large enough red shift for our magnetic trapping to be effective) by a few MHz. We are working now to determine if this is the case, and if so how we can address the issue. My work will continue through the spring semester and into summer in an effort to get the MOT working before Dr. Cundiff moves his lab to the University of Michigan. If I am successful, I will then help Dr. Lomsadze conduct his experiments however I can.

### **References**

- [1] Tianhao Zhang, Irina Kuznetsova, Torsten Meier, Xiaoqin Li, Richard P. Mirin, Peter Thomas, and Steven T. Cundiff. *Polarization Dependent Optical 2D Fourier Transform Spectroscopy of Semiconductors*. Proc. Natl. Acad. Sci. U.S.A. **104**, 14227-14232 (2007)

- [2] “Press Release: The 1997 Nobel Prize in Physics”. [Nobelprize.org](http://www.nobelprize.org/nobel_prizes/physics/laureates/1997/press.html). Nobel Media AB 2014 Web 16. Dec 2014 <  
[http://www.nobelprize.org/nobel\\_prizes/physics/laureates/1997/press.html](http://www.nobelprize.org/nobel_prizes/physics/laureates/1997/press.html)>
- [3] John R. Taylor, Chris D. Zafiratos, and Michael A. Dubson. “*Modern Physics for Scientists and Engineers*”. (Upper Saddle River, NJ: Prentice Hall Publishing 2004). 34-36.
- [4] Stefan Lieder. “*Magneto Optical Trap*”. (2007). Lab course FP20.
- [5] Eugene Hecht. “*Optics – Third Edition*”. (Reading, Massachusetts: Addison-Wesley, 1998). 55-56.
- [6] Adela Marian. “*Direct Frequency Comb Spectroscopy for Optical Frequency Metrology and Coherent Interactions*”. (2005). JILA Thesis. Web 17 Dec. 2014. <[https://jila.colorado.edu/sites/default/files/assets/files/publications/marian\\_thesis.pdf](https://jila.colorado.edu/sites/default/files/assets/files/publications/marian_thesis.pdf)>
- [7] Griffiths, David J. “*Introduction to Quantum Mechanics – Second Edition*”. (Upper Saddle River, NJ: Prentice Hall Publishing, 2005). 277-283.
- [8] Carl Wieman, Gwen Flowers, and Sarah Gilbert. “*Inexpensive Laser Cooling and Trapping Experiment for Undergraduate Laboratories*” –Am. J. Phys. 63 (4). (April 1995).
- [9] Behr, J.A. et. Al. “*Standard Model tests with trapped radioactive atoms*” – J. Phys. G36 (2009).
- [10] Azmoun, Bob, Metcalf, Harold, Metz, Susan. “*Recipe For Locking An Extended Cavity Diode Laser From The Ground Up*”. Stonybrook University. Web 10 Mar. 2015. <http://laser.physics.sunysb.edu/~bazmoun/RbSpectroscopy/>
- [11] MacAdam, K.B., Steinbach A., Wieman C. “*A narrow band tunable diode laser system with grating feedback and a saturated absorption spectrometer for Cs and Rb*” –Am. J. Phys. 60, 1098-1111 (1992).
- [12] Stubbs, Paul L. “*Laser Locking with Doppler Free Saturated Absorption Spectroscopy*” (2010). Web 17 Dec. 2014 <  
<http://physics.wm.edu/Seniorthesis/SeniorThesis2010/stubbsthesis.pdf>>. 3-7.

- [13] “*Saturated Absorption Spectroscopy Systems*”. THORLABS (2014). Web 17 Dec. 2014  
[https://www.thorlabs.com/NewGroupPage9.cfm?ObjectGroup\\_ID=5616](https://www.thorlabs.com/NewGroupPage9.cfm?ObjectGroup_ID=5616)